

Title

Identifying gene-gene interactions that are highly associated with four quantitative lipid traits across multiple cohorts

Rishika De¹, Shefali S. Verma², Emily Holzinger², Molly Hall², Amber Burt³, David S. Carrell⁴, David R. Crosslin⁵, Gail P. Jarvik^{3,5}, Helena Kuivaniemi⁶, Iftikhar J. Kullo⁷, Leslie A. Lange⁸, Matthew B. Lanktree⁹, Eric B. Larson⁴, Kari E. North¹⁰, Alex P. Reiner¹¹, Vinicius Tragante^{12,13}, Gerard Tromp⁶, James G. Wilson¹⁴, Folkert W. Asselbergs^{12,15,16}, Fotios Drenos^{17,18}, Jason H. Moore¹⁹, Marylyn D. Ritchie^{2*}, Brendan Keating^{20,21*}, Diane Gilbert-Diamond^{22,23*}

¹Department of Genetics, Geisel School of Medicine at Dartmouth, Hanover, NH, USA

²The Center for Systems Genomics, The Pennsylvania State University, University Park, PA, USA

³Division of Medical Genetics, Department of Medicine, University of Washington, Seattle, WA, USA

⁴Group Health Research Institute, Seattle, WA, USA

⁵Department of Genome Sciences, University of Washington, Seattle, WA, USA

⁶Division of Molecular Biology and Human Genetics, Department of Biomedical Sciences, Faculty of Medicine and Health Sciences, Stellenbosch University, Tygerberg, 7505, South Africa

⁷Division of Cardiovascular Diseases, Mayo Clinic, Rochester, MN, USA

⁸Department of Genetics, University of North Carolina School of Medicine at Chapel Hill, Chapel Hill, NC, USA

⁹Departments of Medicine and Biochemistry, Schulich School of Medicine and Dentistry, University of Western Ontario, London, Ontario, Canada

¹⁰Department of Epidemiology, School of Public Health, University of North Carolina at Chapel Hill, Chapel Hill, NC, USA

¹¹Division of Public Health Sciences, Fred Hutchinson Cancer Research Center, Seattle, WA, USA

¹²Department of Cardiology, Division Heart and Lungs, University Medical Center Utrecht, Utrecht, The Netherlands

¹³Department of Medical Genetics, Biomedical Genetics, University Medical Center, Utrecht, The Netherlands

¹⁴Department of Physiology and Biophysics, University of Mississippi Medical Center, Jackson, MS, USA

¹⁵Institute of Cardiovascular Science, University College London, 222 Euston Road, London, NW1 2DA, UK

¹⁶Durrer Center for Cardiogenetic Research, ICIN-Netherlands Heart Institute, Utrecht, The Netherlands

¹⁷MRC Integrative Epidemiology Unit, School of Social and Community Medicine, University of Bristol, Oakfield House, Oakfield Grove, Bristol, UK

¹⁸Centre for Cardiovascular Genetics, Institute of Cardiovascular Science, University College London, London, UK

¹⁹Institute for Biomedical Informatics, The Perelman School of Medicine, University of Pennsylvania, Philadelphia, PA, USA

²⁰University Medical Center Utrecht, Utrecht, The Netherlands

²¹The Children's Hospital of Philadelphia, Philadelphia, PA, USA

²²Institute for Quantitative Biomedical Sciences at Dartmouth, Hanover, NH, USA

²³Department of Epidemiology, Geisel School of Medicine at Dartmouth, Hanover, NH, USA

*Corresponding authors

mdr23@psu.edu, Ph: 570 214 7579 (MDR)

bkeating@mail.med.upenn.edu, Ph: 267 760 4507 (BK)

Diane.Gilbert-Diamond@dartmouth.edu, Ph: 603 653 3362 (DGD)

Abstract

Genetic loci explain only 25-30% of the heritability observed in plasma lipid traits. *Epistasis*, or gene-gene interactions may contribute to a portion of this *missing heritability*. Using genetic data from five NHLBI cohorts of 24,837 individuals, we combined the use of the quantitative multifactor dimensionality reduction (QMDR) algorithm with two SNP filtering methods to exhaustively search for SNP-SNP interactions that are associated with HDL cholesterol (HDL-C), LDL cholesterol (LDL-C), total cholesterol (TC) and triglycerides (TG). SNPs were filtered either on the strength of their independent effects (main effect filter) or the prior knowledge supporting a given interaction (Biofilter). After the main effect filter, QMDR identified 20 SNP-SNP models associated with HDL-C, 6 associated with LDL-C, 3 associated with TC, and 10 associated with TG (permutation P -value < 0.05). With the use of Biofilter, we identified 2 SNP-SNP models associated with HDL-C, 3 associated with LDL-C, 1 associated with TC and 8 associated with TG (permutation P -value < 0.05). In an independent dataset of 7,502 individuals from the eMERGE network, we replicated 14 of the interactions identified after main effect filtering: 11 for HDL-C, 1 for LDL-C and 2 for TG. We also replicated 23 of the interactions found to be associated with TG after applying Biofilter. Prior knowledge supports the possible role of these interactions in the genetic etiology of lipid traits. This study also presents a computationally efficient pipeline for analyzing data from large genotyping arrays and detecting SNP-SNP interactions that are not primarily driven by strong main effects.

Keywords

Epistasis, gene-gene interactions, lipid disorders, cholesterol, MDR

Introduction

Plasma lipid and lipoprotein levels are a major risk factor for cardiovascular disease (CVD), the leading cause of death in the world (Arsenault et al. 2011; World Health Organization 2014). In 2012, approximately one-third of all global deaths were caused by CVD (Deaton et al. 2011; World Health Organization 2014). Moreover, CVD no longer remains a disease associated with industrialized nations. With increasing urbanization around the world, 80% of global CVD-related deaths occur in low- and middle-income countries and the World Health Organization estimates global CVD-related deaths to reach 22.2 million by 2030 (World Health Organization 2014).

Although lipid levels can be influenced by factors such as age, sex, body mass index (BMI), environmental factors and lifestyle choices including diet, they can be influenced by genetic factors as well (Heller et al. 1993). Lipid traits such as high density lipoprotein cholesterol (HDL-C), low density lipoprotein cholesterol (LDL-C), total cholesterol (TC) and triglyceride (TG) levels have been shown to have heritability estimates ranging between 40% to 60% (Weiss et al. 2006).

Various genetic loci associated with lipid traits have been identified by genome-wide association studies (GWAS); however, these loci only explain 25-30% of the heritability observed in plasma lipid traits (Kathiresan et al. 2009; Teslovich et al. 2010). *Epistasis*,

or interactions between genes, may help to explain a portion of the *missing heritability* of lipid traits (Manolio et al. 2009) and studies are needed to examine the genomic context of single nucleotide polymorphisms (SNPs) by specifically searching for non-linear interactions between them (Eichler et al. 2010).

Exhaustively searching for interactions between SNPs in large datasets generated with genotyping arrays leads to a prohibitive number of statistical tests and is computationally expensive (Moore et al. 2010). Although other approaches such as BOOST and MB-MDR are significant alternatives that enable researchers to perform a genome-wide analysis for gene-gene interactions – they were not an ideal fit for the purposes of this study. For example, the BOOST method can only analyze binary phenotypes (Wan et al. 2010). Additionally, the MB-MDR method relies on performing a chi-square test, which can be ineffective when contingency tables become sparse (Calle et al. 2010). Researchers have also reported on the computational intensity required to perform a genome wide screening using MB-MDR (Gundlach et al. 2016).

In this study, we addressed these bioinformatics challenges by applying SNP-filtering methods along with the quantitative multifactor dimensionality reduction (QMDR) machine learning algorithm to the analysis of lipid traits for the first time. We aimed to identify interactions between SNPs that are associated with four lipids traits (HDL-C, LDL-C, TC and TG) across five National Heart, Lung and Blood Institute (NHLBI) study cohorts. These SNPs have also been analyzed as part of a previous large-scale study aimed at identifying independent signals associated with multiple lipid traits using regression methods. This study identified 21 novel loci that had not been found to be

associated with lipid traits before. The study also replicated a large number of previously implicated signals associated with lipid traits (Asselbergs et al. 2012).

Results

Main effect filter

The main effect filter resulted in a final list of 486 markers to be tested for SNP-SNP interactions for HDL-C, 462 markers for LDL-C, 571 markers for TC and 502 markers for TG. After QMDR analysis, at a permutation P -value < 0.05 , we identified 20 SNP-SNP interaction models that were associated with HDL-C (Table 1), 6 SNP-SNP interaction models associated with LDL-C (Table 1), 3 SNP-SNP interaction models associated with TC (Table 1), and 10 SNP-SNP models associated with TG (Table 1).

Table 1 Results from QMDR association analysis of Main effect filter SNPs for lipid traits

SNP1	Chr:bp	Gene1	SNP1 Function	SNP1 Main Effect P-Value	SNP2	Chr:bp	Gene2	SNP2 Function	SNP2 Main Effect P-Value	Interaction Permuted P-Value
HDL-C										
rs4783961	16:55552395	<i>CETP</i>	Exonic	1.286E-51	rs1800775	16:55552737	<i>CETP</i>	Exonic	2.46E-196	< 0.00001
rs12720918	16:55551713	<i>CETP</i>	Exonic	3.15E-79	rs158477	16:55565111	<i>CETP</i>	Intronic	3.747E-12	< 0.00001
rs4783961	16:55552395	<i>CETP</i>	Exonic	1.286E-51	rs1864163	16:55554734	<i>CETP</i>	Intronic	5.33E-185	< 0.00001
rs12720918	16:55551713	<i>CETP</i>	Exonic	3.15E-79	rs4783961	16:55552395	<i>CETP</i>	Exonic	1.286E-51	< 0.00001
rs1864163	16:55554734	<i>CETP</i>	Intronic	5.33E-185	rs4784744	16:55568686	<i>CETP</i>	Intronic	1.86E-36	< 0.00005
rs12708967	16:55550712	<i>CETP</i>	Exonic	8.5E-102	rs820299	16:55557785	<i>CETP</i>	Intronic	2.457E-16	< 0.00024
rs12447924	16:55551693	<i>CETP</i>	Exonic	3.48E-18	rs9939224	16:55560233	<i>CETP</i>	Intronic	2.1E-172	< 0.00031
rs4783961	16:55552395	<i>CETP</i>	Exonic	1.286E-51	rs158477	16:55565111	<i>CETP</i>	Intronic	3.747E-12	< 0.00087
rs1864163	16:55554734	<i>CETP</i>	Intronic	5.33E-185	rs158477	16:55565111	<i>CETP</i>	Intronic	3.747E-12	< 0.00104
rs1864163	16:55554734	<i>CETP</i>	Intronic	5.33E-185	rs820299	16:55557785	<i>CETP</i>	Intronic	2.457E-16	0.00405
rs4783961	16:55552395	<i>CETP</i>	Exonic	1.286E-51	rs9939224	16:55560233	<i>CETP</i>	Intronic	2.1E-172	< 0.00525
rs1800775	16:55552737	<i>CETP</i>	Exonic	2.46E-196	rs820299	16:55557785	<i>CETP</i>	Intronic	2.457E-16	< 0.0083
rs12744291	1:66135559	<i>PDE4B</i>	Intronic	0.002352	rs1010554	3:52517959	<i>STAB1</i>	Intronic	0.0004028	< 0.00873
rs230541	4:103716823	<i>NFKB1</i>	Intronic	0.001379	rs4935047	10:54200073	<i>MBL2</i>	Intronic	0.002622	0.01116
rs12976922	19:60562163	<i>COX6B2</i>	Exonic	0.006489	rs2952101	X:14768515	<i>FANCB</i>	Intronic	0.001637	< 0.0119
rs9644636	8:19869176	<i>LPL</i>	Exonic	3.031E-12	rs7013777	8:19922636	<i>LPL</i>	-	7.58E-26	< 0.01719

rs9939224	16:55560233	<i>CETP</i>	Intronic	2.1E-172	rs4784744	16:55568686	<i>CETP</i>	Intronic	1.86E-36	0.01843
rs599839	1:109623689	<i>PSRC1</i>	Exonic	1.967E-07	rs2952101	X:14768515	<i>FANCB</i>	Intronic	0.001637	0.02954
rs12708967	16:55550712	<i>CETP</i>	Exonic	8.5E-102	rs158477	16:55565111	<i>CETP</i>	Intronic	3.747E-12	0.03023
rs3870336	3:49532861	<i>DAG1</i>	Intronic	0.001736	rs6641322	X:149494622	<i>IDS</i>	Intronic	0.005715	< 0.04418

LDL-C

rs157580	19:50087106	<i>TOMM40</i>	Intronic	5.623E-38	rs439401	19:50106291	<i>APOE</i>	Intronic	0.002661	< 0.00522
rs17435152	7:40568630	<i>C7orf10</i>	Intronic	0.004781	rs3764261	16:55550825	<i>CETP</i>	-	0.000001483	0.00743
rs157580	19:50087106	<i>TOMM40</i>	Intronic	5.623E-38	rs405509	19:50100676	<i>APOE</i>	Exonic	1.503E-33	0.00781
rs12811752	12:20469072	<i>PDE3A</i>	Intronic	0.00391	rs1469713	19:19389806	<i>GATAD2A</i>	Intronic	0.00007551	< 0.01293
rs480780	13:32505319	<i>KL</i>	Intronic	0.00008468	rs2965174	19:49936855	<i>BCL3</i>	Exonic	0.000003422	0.02482
rs625619	1:55290754	<i>PCSK9</i>	Intronic	0.000398	rs3764261	16:55550825	<i>CETP</i>	-	0.000001483	0.03809

TC

rs693	2:21085700	<i>APOB</i>	Exonic	2.057E-44	rs661665	2:21118646	<i>APOB</i>	Intronic	0.0005396	< 0.00835
rs12898801	15:56585846	<i>LIPC</i>	Intronic	0.009846	rs953065	15:87203929	<i>ACAN</i>	Intronic	0.002909	< 0.01297
rs10744777	12:110717401	<i>ALDH2</i>	Intronic	0.002676	rs749767	16:31031908	<i>BCKDK</i>	Exonic	0.003476	0.01975

TG

rs2075295	11:116133611	<i>BUD13</i>	Intronic	0.000001359	rs6589568	11:11617594 8	<i>APOA5</i>	-	5.402E-20	< 0.00001
rs4938303	11:116090197	<i>BUD13</i>	-	9.893E-73	rs180327	11:11612886 9	<i>BUD13</i>	Intronic	1.75E-45	< 0.00001
rs180327	11:116128869	<i>BUD13</i>	Intronic	1.75E-45	rs2075295	11:11613361 1	<i>BUD13</i>	Intronic	0.000001359	< 0.00007
rs180327	11:116128869	<i>BUD13</i>	Intronic	1.75E-45	rs10750097	11:11616925 0	<i>APOA5</i>	Exonic	3.56E-97	< 0.00027

rs11216129	11:116125466	<i>BUD13</i>	Intronic	0.000005043	rs10750097	11:11616925 0	<i>APOA5</i>	Exonic	3.56E-97	< 0.00516
rs609526	1:228375529	<i>GALNT2</i>	Intronic	0.002831	rs12257915	10:90982709	<i>LIPA</i>	Intronic	0.005381	< 0.03321
rs2075295	11:116133611	<i>BUD13</i>	Intronic	0.000001359	rs10750097	11:11616925 0	<i>APOA5</i>	Exonic	3.56E-97	< 0.03351
rs4938303	11:116090197	<i>BUD13</i>	-	9.893E-73	rs6589568	11:11617594 8	<i>APOA5</i>	-	5.402E-20	< 0.03379
rs174455	11:61412693	<i>FADS3</i>	Intronic	3.106E-07	rs689243	11:11622790 3	<i>KIAA0999</i>	Intronic	8.632E-24	< 0.03789
rs180327	11:116128869	<i>BUD13</i>	Intronic	1.75E-45	rs618923	11:11615936 9	<i>ZNF259</i>	Intronic	6.708E-20	< 0.03833

Signals reached a permutation P-value < 0.05. SNPs have been mapped to their corresponding genes using dbSNP (build 139). SNP1 and SNP2 indicate the individual SNPs within a given SNP-SNP interaction model. Chromosomal location of SNPs is noted in the following format - Chromosome:Base pair. Functional consequences were identified using dbSNP. Information for some SNPs was not available. P-values were calculated from a distribution built from 1000 permutations.

In the case of HDL-C, a large number of the identified SNP-SNP models represent intra-genic interactions within *CETP*. Fig. 1 shows the underlying LD structure of these interactions. None of the interacting SNPs were in strong LD ($r^2 > 0.8$). Moreover, none of the identified pairwise interactions for each of the quantitative lipid traits exhibited strong LD (Figs. S1-3).

Biofilter

The Biofilter procedure resulted in a final list of 1,811 markers (22,487 SNP-SNP models) for HDL-C, 1,812 markers (22,491 SNP-SNP models) for LDL-C, 1,812 markers (22,454 SNP-SNP models) for TC and 1,811 markers (22,487 SNP-SNP models) for TG. QMDR analysis identified 14 significant SNP-SNP models with a permutation P -value < 0.05 : 2 SNP-SNP models associated with HDL-C, 3 SNP-SNP models associated with LDL-C, 1 SNP-SNP model associated with TC and 8 SNP-SNP models associated with TG (Table 2). None of the interacting SNPs were found to be in strong LD in this case as well (Figs. S4-7).

Table 2 Results from QMDR association analysis of Biofilter SNPs for lipid traits

SNP1	Chr:bp	Gene1	SNP1 Function	SNP2	Chr:bp	Gene2	SNP2 Function	Permuted P-Value
HDL-C								
rs17496549	6:32517686	<i>HLA-DRA</i>	Intronic	rs615672	6:32682149	<i>HLA-DRB1</i>	-	< 0.01178
rs549888	6:33660180	<i>GGNBP1</i>	Intronic	rs7240326	18:59068331	<i>BCL2</i>	Intronic	0.0404
LDL-C								
rs39499	8:90839744	<i>RIPK2</i>	Intronic	rs751919	16:49333246	<i>CYLD</i>	Intronic	0.03262
rs12693591	2:191568747	<i>STAT1</i>	Intronic	rs8072566	17:37729889	<i>STAT3</i>	Intronic	0.04211
rs2066795	2:191560142	<i>STAT1</i>	Intronic	rs8074524	17:37723124	<i>STAT3</i>	Intronic	< 0.04788
TC								
rs4725431	7:151104112	<i>PRKAG2</i>	Intronic	rs10875915	12:47716361	<i>MLL2</i>	Intronic	< 0.04276
TG								
rs9521510	13:109224872	<i>IRS2</i>	Intronic	rs2860184	19:7238748	<i>INSR</i>	Intronic	< 0.00079
rs9521510	13:109224872	<i>IRS2</i>	Intronic	rs6510976	19:7217944	<i>INSR</i>	Intronic	< 0.00289
rs2075110	7:55186653	<i>EGFR</i>	Intronic	rs4789172	17:70853307	<i>GRB2</i>	Intronic	< 0.00385
rs4773088	13:109219885	<i>IRS2</i>	Intronic	rs4804404	19:7169382	<i>INSR</i>	Intronic	< 0.00401
rs7999797	13:109224001	<i>IRS2</i>	Intronic	rs8109559	19:7122629	<i>INSR</i>	Intronic	0.01758
rs4771646	13:109225180	<i>IRS2</i>	Intronic	rs4804404	19:7169382	<i>INSR</i>	Intronic	< 0.02007
rs1729409	11:116178978	<i>APOA5</i>	-	rs11216162	11:116233487	<i>KIAA0999</i>	Intronic	< 0.02063
rs7999797	13:109224001	<i>IRS2</i>	Intronic	rs7252268	19:7121505	<i>INSR</i>	Intronic	< 0.03164

Signals reached a permutation P-value < 0.05. SNPs have been mapped to their corresponding genes using dbSNP (build 139). SNP1 and SNP2 indicate the individual SNPs within a given SNP-SNP interaction model. Chromosomal location of SNPs is noted in the following format - Chromosome:Base pair. P-values were calculated from a distribution built from 1000 permutations.

Replication analyses

After following an identical QMDR analysis procedure, we were able to replicate SNP-SNP models in the eMERGE dataset at a permutation P -value threshold of 0.05. Eleven main effect filtered SNP-SNP models were replicated for HDL-C, 1 main effect filtered SNP-SNP model for LDL-C and 2 such models for TG (Table 3). Additionally, 23 Biofilter SNP-SNP models replicated for TG (Table 3).

Added variance in lipid traits explained

The adjusted R^2 values and associated likelihood ratio test P -values are as follows:
Main effect filter: HDL full = 0.03355578, HDL reduced = 0.03181211 (P -value = 0.01);
LDL full = 0.01514733, LDL reduced = 0.01355952 (P -value = 0.002); TG full =
0.007837119, TG reduced = 0.00765267 (P -value = 0.2). Biofilter: TG full = -
0.001432491, TG reduced = -0.0005782882 (P -value = 0.9). Although in most cases the
inclusion of interacting SNPs showed an increase in the variance explained, the
difference was statistically significant for the HDL and LDL main effect analyses.

Table 3 Results from QMDR association analysis of main effect and Biofilter SNP-SNP models replicated in eMERGE dataset

Rank	Model	SNP1	Chr:bp	Gene1	SNP2	Chr:bp	Gene2	Permuted P-Value
Main effect filter: HDL Cholesterol Levels								
1	rs4783961,rs1800775	rs4783961	16:55552395	<i>CETP</i>	rs1800775	16:55552737	<i>CETP</i>	< 0.00001
2	rs4783961,rs3816117	rs4783961	16:55552395	<i>CETP</i>	rs3816117	16:55553659	<i>CETP</i>	< 0.00001
3	rs4783961,rs1532624	rs4783961	16:55552395	<i>CETP</i>	rs1532624	16:55562980	<i>CETP</i>	< 0.00001
4	rs4783961,rs1532625	rs4783961	16:55552395	<i>CETP</i>	rs1532625	16:55562802	<i>CETP</i>	< 0.00001
5	rs4783961,rs7205804	rs4783961	16:55552395	<i>CETP</i>	rs7205804	16:55562390	<i>CETP</i>	< 0.00001
6	rs4783961,rs711752	rs4783961	16:55552395	<i>CETP</i>	rs711752	16:55553712	<i>CETP</i>	< 0.00001
7	rs4783961,rs708272	rs4783961	16:55552395	<i>CETP</i>	rs708272	16:55553789	<i>CETP</i>	< 0.00001
8	rs1864163,rs289717	rs1864163	16:55554734	<i>CETP</i>	rs289717	16:55566889	<i>CETP</i>	< 0.00004
9	rs1864163,rs4784744	rs1864163	16:55554734	<i>CETP</i>	rs4784744	16:55568686	<i>CETP</i>	< 0.00004
10	rs1864163,rs291044	rs1864163	16:55554734	<i>CETP</i>	rs291044	16:55568953	<i>CETP</i>	< 0.00004
11	rs4783961,rs1864163	rs4783961	16:55552395	<i>CETP</i>	rs1864163	16:55554734	<i>CETP</i>	< 0.00229
Main effect filter: LDL Cholesterol Levels								
1	rs157580,rs405509	rs157580	19:50087106	<i>TOMM40</i>	rs405509	19:50100676	<i>APOE</i>	< 0.00488
Main effect filter: Triglyceride Levels								
1	rs180327,rs618923	rs180327	11:116128869	<i>BUD13</i>	rs618923	11:116159369	<i>ZNF259</i>	< 0.31483
2	rs180326,rs618923	rs180326	11:116129913	<i>BUD13</i>	rs618923	11:116159369	<i>ZNF259</i>	< 0.33204
Biofilter: Triglyceride Levels								
1	rs9521510,rs6510976	rs9521510	13:109224872	<i>IRS2</i>	rs6510976	19:7217944	<i>INSR</i>	< 0.01014
2	rs35612086,rs6510976	rs35612086	13:109244865	<i>IRS2</i>	rs6510976	19:7217944	<i>INSR</i>	< 0.01155
3	rs36092351,rs6510976	rs36092351	13:109246741	<i>IRS2</i>	rs6510976	19:7217944	<i>INSR</i>	< 0.01163
4	rs2117455,rs6510976	rs2117455	13:109241895	<i>IRS2</i>	rs6510976	19:7217944	<i>INSR</i>	< 0.01166
5	rs9521517,rs6510976	rs9521517	13:109245638	<i>IRS2</i>	rs6510976	19:7217944	<i>INSR</i>	< 0.01166
6	rs1414316,rs6510976	rs1414316	13:109248190	<i>IRS2</i>	rs6510976	19:7217944	<i>INSR</i>	< 0.01168
7	rs9521510,rs6510975	rs9521510	13:109224872	<i>IRS2</i>	rs6510975	19:7217878	<i>INSR</i>	< 0.01259

8	rs9515119,rs6510975	rs9515119	13:109207337	<i>IRS2</i>	rs6510975	19:7217878	<i>INSR</i>	< 0.01643
9	rs9515119,rs6510976	rs9515119	13:109207337	<i>IRS2</i>	rs6510976	19:7217944	<i>INSR</i>	< 0.01657
10	rs2289046,rs6510975	rs2289046	13:109205907	<i>IRS2</i>	rs6510975	19:7217878	<i>INSR</i>	< 0.01657
11	rs2289047,rs6510975	rs2289047	13:109205816	<i>IRS2</i>	rs6510975	19:7217878	<i>INSR</i>	< 0.01657
12	rs2289046,rs6510976	rs2289046	13:109205907	<i>IRS2</i>	rs6510976	19:7217944	<i>INSR</i>	0.01680
13	rs2289047,rs6510976	rs2289047	13:109205816	<i>IRS2</i>	rs6510976	19:7217944	<i>INSR</i>	0.01680
14	rs4771649,rs6510976	rs4771649	13:109248514	<i>IRS2</i>	rs6510976	19:7217944	<i>INSR</i>	< 0.01709
15	rs35612086,rs6510975	rs35612086	13:109244865	<i>IRS2</i>	rs6510975	19:7217878	<i>INSR</i>	< 0.02214
16	rs36092351,rs6510975	rs36092351	13:109246741	<i>IRS2</i>	rs6510975	19:7217878	<i>INSR</i>	< 0.02220
17	rs2117455,rs6510975	rs2117455	13:109241895	<i>IRS2</i>	rs6510975	19:7217878	<i>INSR</i>	< 0.02223
18	rs9521517,rs6510975	rs9521517	13:109245638	<i>IRS2</i>	rs6510975	19:7217878	<i>INSR</i>	0.02223
19	rs1414316,rs6510975	rs1414316	13:109248190	<i>IRS2</i>	rs6510975	19:7217878	<i>INSR</i>	< 0.02225
20	rs2075110,rs4789172	rs2075110	7:55186653	<i>EGFR</i>	rs4789172	17:70853307	<i>GRB2</i>	< 0.02793
21	rs4771649,rs6510975	rs4771649	13:109248514	<i>IRS2</i>	rs6510975	19:7217878	<i>INSR</i>	0.03304
22	rs2075109,rs4789172	rs2075109	7:55186397	<i>EGFR</i>	rs4789172	17:70853307	<i>GRB2</i>	0.04293
23	rs9521518,rs6510976	rs9521518	13:109251997	<i>IRS2</i>	rs6510976	19:7217944	<i>INSR</i>	0.04882

Shown here are models that reached a permutation P-value < 0.05 in the replication dataset. SNPs have been mapped to their corresponding genes using dbSNP (build 139). SNP1 and SNP2 indicate the individual SNPs within a given SNP-SNP interaction model. . Chromosomal location of SNPs is noted in the following format - Chromosome:Base pair. P-values were calculated from a distribution built from 1000 permutations.

Discussion

Although many researchers acknowledge the need for embracing the complexity of the genotype-phenotype relationship by studying gene-gene interactions, exploring epistasis in large genotyping arrays presents a biostatistical and computational challenge. These challenges call for new computational methods since more traditional approaches such as general linear models may have limited power when modeling high-dimensional data. The use of SNP-filtering methods has been presented as a suitable solution to ease the computational burden of exhaustively searching for all possible interactions between large numbers of SNPs (Moore et al. 2010).

In our analyses, we combined genotypic and phenotypic information for four quantitative lipid traits – HDL-C, LDL-C, TC and TG – for 24,837 individuals from five study cohorts. We reduced the number of interactions tested by filtering SNPs either based on the strength of their independent effects or the strength of relevant prior biological knowledge. Filtered SNPs were tested for two-way SNP-SNP interactions associated with each quantitative lipid trait using QMDR.

SNPs tested from the main effect filter and Biofilter methods showed only 2-3% overlap in each of the four lipid traits (HDL: 35 SNPs, LDL: 40 SNPs, TC: 64 SNPs, TG: 52 SNPs). None of these overlapping SNPs were part of the SNP x SNP interactions replicated in the eMERGE dataset. However, two biological pathways highlighted by these overlapping SNPs were identified by our replicated genetic interactions as well. For

example, there is overlap in the hepatic insulin signaling pathway and its relationship with lipogenesis, as highlighted by INSR and IRS2. The growth factor signaling relationship between EGFR and GRB2 is also captured by the overlapping SNPs.

We also evaluated how much of the explained phenotypic variance of the four quantitative lipid traits could be increased by the SNP-SNP interactions we replicated. We found statistically significant increases in the variance explained for HDL (5.5%) and LDL (11.7%) in our main effect filter analyses, beyond what is explained by the main effects of SNPs within these replicated interactions.

Below we highlight the potential biological functions for several genes at or near the identified interacting SNPs. Further details regarding the biological roles and functions associated with all genes at or near these interactions are listed in Table S1.

HDL-C

In our analysis, the 25 total SNPs that we identified to interact significantly with each other, were in or near 15 genes. Ten SNPs were located at or near *CETP*, which is involved in the transfer of cholesteryl ester from HDL to other lipoproteins (Barter et al. 2003). Moreover, we identified 12 intra-genic interactions between independent SNPs within the *CETP* region (Table 1). Three of the original intra-genic *CETP* interactions (interactions 1, 9 and 11 in Table 3) and 8 additional LD expanded interactions were replicated in the eMERGE dataset. Though the impact of these intra-genic regions on

HDL-C is unknown, they may act through regulatory or epigenetic mechanisms (Soto-Ramírez et al. 2013; Olsson et al. 2014).

Some of the other identified genes also have well studied roles in lipid and cholesterol metabolism such as – *LPL* and *PSRC1* (Brown et al. 1989; Kuivenhoven et al. 1997). Both genes were identified in interactions in the discovery dataset only. Two SNPs were at or near *LPL*; mutations in *LPL* are linked to various disorders of lipoprotein metabolism and have been previously reported to alter HDL-C levels (Reymer et al. 1995; Wittekoek et al. 1998). We also identified one intra-genic interaction within *LPL* (Table 1). Lastly, 1 SNP was near *PSRC1*. Variations within *PSRC1* have also been shown be associated with cholesterol traits in previous GWA studies (Kathiresan et al. 2008a; Ma et al. 2010; Voight et al. 2012).

The IMP network of genes represented in main effect filtered SNP-SNP models associated with HDL-C, includes genes from replicated and non-replicated interactions. The interaction between *PSRC1* with *BRCA1* via *AURKA* in this network, highlights a potentially interesting biological connection between dyslipidemia and breast cancer (Fig. 2a). High cholesterol has been highlighted as a risk factor for breast cancer and various mechanisms linking the two diseases have been hypothesized and studied (Nelson et al. 2014). The interaction between *PSRC1* and *AURKA* in this network reflects their well-known role in spindle organization. There was also strong support for the interaction between *AURKA* and *BRCA1*. This is not surprising since, *AURKA* is a known to be an

activator of Akt (Yao et al. 2009) – a kinase involved in tumor cell growth (Paplomata and O'Regan 2014).

LDL-C

We identified 16 total SNPs to interact significantly with each other, located in or near 13 genes. These findings included two SNP-SNP models representing interactions between the genes *TOMM40* and *APOE*. One of these interaction models replicated in the eMERGE dataset (Table 3). The *TOMM40/APOE-C1-C2-C4* gene cluster has been shown to affect LDL-C levels previously (Klos et al. 2008; Middelberg et al. 2011). In the IMP network built from SNP-SNP models identified after main effect filtering, there is strong support for the interaction between *TOMM40* and *FARSA*, which encodes for the alpha subunit of a phenylalanyl-tRNA synthetase (Fig. 2b). *FARSA* is also involved in a protein-protein interaction with the ECSIT signaling integrator, which in turn interacts with *APOE*. Furthermore, *APOE* interacts with *LDLR* in the network, highlighting their shared role in sterol transport and cholesterol homeostasis (Fig. 2b). *LDLR*, which encodes for the LDL receptor, also interacts with *PCSK9* in the network since both genes share a role in cholesterol homeostasis (Fig. 2b). *PCSK9* binds *LDLR* and promotes degradation of the LDL receptor either in the lysosome or in the liver (Cao et al. 2011). Hence, due to its inhibitory role with *LDLR*, it has emerged as an attractive drug target for hypercholesterolemia (Akram et al. 2010).

The IMP network also had an enrichment of processes such as - cholesterol and lipid homeostasis, cholesterol transport, regulation of plasma lipoprotein particle levels, plasma lipoprotein particle clearance, and low density lipoprotein particle receptor catabolic process. The genes involved in these processes included *APOE*, *CETP* and *PCSK9*. SNPs within these genes have been previously found to be associated with LDL-C (Talmud et al. 2009).

Total Cholesterol

There were 3 SNP-SNP interactions that were significantly associated with TC after main effect filtering. An intra-genic interaction within *APOB* was most significantly associated with TC after main effect filtering, although it did not replicate in the eMERGE dataset. Mutations within *APOB* can cause familial defective apolipoprotein B-100 (FDB) – an inherited form of hypercholesterolemia (Hooper et al. 2005). The protein encoded by this gene forms the building block for various types of low-density lipoproteins. It is also involved in cholesterol homeostasis and sterol transport. Researchers have also found a polymorphism on this gene to increase LDL-C levels (Benn et al. 2005).

There was one significant SNP-SNP interaction associated with TC after Biofilter filtering which also did not replicate in the eMERGE dataset. The gene-gene interaction between *MLL2* and *PRKAG2* highlights biological processes such as histone methylation, protein alkylation and protein methylation (Wong et al. 2012). *MLL2*, which codes for a

mixed-lineage leukemia histone methylase, contributes to the activation of SR-B1. SR-B1 is a class-B type-1 scavenger receptor responsible for maintaining blood cholesterol levels (Ansari et al. 2012). *PRKAG2* encodes for the regulatory $\gamma 2$ subunit of an AMP-activated protein kinase. Homozygotes of an intronic SNP within this gene have been found to have elevated serum concentrations of TC and TG (Xu et al. 2005).

Triglycerides

We found an interaction between *BUD13* and *ZNF259*. This interaction and an LD-expanded SNP-SNP model representing it were replicated in the eMERGE dataset (Table 3). An interaction between variants on these two genes has been found to be associated with TG and TC before (Aung et al. 2014). Moreover, many studies have found polymorphisms within *BUD13* to be associated with TG (Kathiresan et al. 2008b; Waterworth et al. 2010; Aung et al. 2014). *BUD13* encodes for the BUD13 homolog protein. It is part of the RES complex that was originally identified as a splicing factor in yeast and shown to affect nuclear pre-mRNA retention (Brooks et al. 2009).

Six of the eight SNP-SNP interactions associated with TG after Biofilter filtering, represent an interaction between the genes *INSR* and *IRS2*. Twenty-one models representing this SNP-SNP interaction were identified in the eMERGE dataset as well (Table 3). This included two of the original SNP-SNP interactions between these genes (interactions 1 and 20 in Table 3). *INSR* encodes for the insulin receptor, which works with the *IRS2* molecule in hepatic insulin signaling. Insulin is also known to activate

lipogenesis within the liver. Moreover, an inverse relationship between *IRS2* and *SREBP-1* gene expression has been demonstrated (Ide et al. 2004). SREBPs are transcription factors that are involved in the expression of various genes involved in the synthesis of triglycerides (Horton et al. 2002).

Strengths and Limitations

Despite the computational and biostatistical challenges of investigating gene-gene interactions in datasets from large genotyping arrays, we have established an efficient analytic framework to overcome the limited power of traditional statistical methods when modeling high-dimensional data. The use of knowledge-based filtering methods within our framework improved our ability to identify biologically relevant interactions in the context of lipid phenotypes.

However, our methods are limited by the strength of the knowledge of gene functions available in public databases. Our replication sample was small which could have decreased our power to replicate the interactions we identified in our discovery dataset.

Additionally, the genetic similarity and the underlying LD structures of our study population and that of the reference groups can affect our genotype imputation results. However, we attempted to address these biases through the use of cosmopolitan reference panels (Verma et al. 2014). Lastly, although the use of SNP-filtering methods have been suggested as a favorable solution for reducing the computational burden of studying

epistasis in such large datasets, they do introduce their own biases into the study, which have been discussed previously (Ritchie 2011).

The use of traditional statistical methods focusing on main effects has been able to explain only a portion of the heritability of lipid traits. We performed a comprehensive analysis by examining gene-gene interactions within four quantitative lipid traits – HDL-C, LDL-C, TC and TG, from five study cohorts. With the use of machine learning algorithms such as QMDR, a targeted gene-centric genotypic chip and SNP-filtering methods, we identified multiple gene-gene interactions associated with these lipid traits. Existing knowledge suggests potentially important roles for these genes in the pathobiology of lipid traits. **Ultimately, the true effect of these interactions will have to be validated at the bench.**

Subjects and Methods

Participating Cohorts

The overall study design is shown in Fig. 3. Genotype and phenotype information was combined from the following studies: Atherosclerosis Risk in Communities (ARIC) (Hill et al. 1989); Coronary Artery Risk Development in Young Adults (CARDIA) (Friedman et al. 1988); Cardiovascular Health Study (CHS) (Fried et al. 1991); Framingham Heart Study (FHS) (Dawber et al. 1951); and Multi-Ethnic Study of Atherosclerosis (MESA)

(Bild et al. 2002) (Table S2), resulting in an initial sample size of 24,837 individuals of self-reported European ancestry.

The eMERGE I-660 dataset was used for replication analyses (McCarty et al. 2011). This dataset was imputed using data from the 1000 Genomes Project (Verma et al. 2014). Detailed information regarding the replication dataset is presented in Table S3.

Phenotypic outcomes measured

HDL-C, LDL-C, TC and TG levels were measured from baseline or first measurement blood samples. All measurements were converted to mmol/L. LDL-C was calculated according to Friedewald's formula (Friedewald et al. 1972):

$$L \sim C - H - kT$$

where C is total cholesterol, H is HDL, L is LDL, T is triglycerides, and k is 0.45 for mmol/L. If TG values were > 4.51 mmol/L, then LDL was treated as a missing value. Additionally, TG values were transformed for normality.

Genotyping and quality control

Study participants in the discovery dataset were genotyped using the gene-centric ITMAT-Broad-CARe (IBC) array. The IBC array contains 47,451 SNPs and it was designed to test $\sim 2,100$ loci that have been implicated in various cardiovascular,

metabolic and inflammatory phenotypes (Keating et al. 2008). SNPs with a genotype missing rate greater than 95%, with an exact test of Hardy-Weinberg equilibrium P -value $< 1.0 \times 10^{-7}$ or a minor allele frequency (MAF) < 0.05 were excluded. Samples with a genotype missing rate greater than 90% were also excluded. This reduced our dataset to 24, 837 individuals and 44,570 SNPs.

Non-founder individuals were also removed from the study population. To check for relatedness between individuals, identity-by-descent (IBD) estimates were calculated using PLINK (Purcell et al. 2007). For each pair of individuals with a $\hat{\pi} > 0.3$, one individual was removed.

Finally, individual datasets with no missing phenotype data were created for each of the lipid outcomes measured. Within each of the datasets, SNPs were further tested for linkage disequilibrium (LD) – a SNP was removed from each pair of SNPs that had an LD (r^2) ≥ 0.6 . Genotypes were also imputed, to ensure there was no missing genotype information. The most common genotype for a given marker was used as the imputed genotype. Further details of the number of SNPs and individuals in each of these datasets can be found in Fig. 3.

Study participants in the replication dataset were from the eMERGE network. The eMERGE network is a consortium of institutions with DNA from biorepositories linked to data from patient electronic medical records (EMR) (Gottesman et al. 2013). The eMERGE set was genotyped with the Illumina660W GWAS platform and further

imputed using 1000 Genomes project data, as described previously (Verma et al. 2014). The replication set consisted of data from the Marshfield Clinic, Northwestern University, Group Health Cooperative, Mayo Clinic, and Vanderbilt University. After QC, the final eMERGE sample size was $n=7,502$ for all lipid traits. Details on quality control and phenotype extractions from the EMR have been published previously (Rasmussen-Torvik et al. 2012). Briefly, each cohort tested for population stratification and relatedness, adjusting accordingly. The minimum variant and sample call rate threshold for all replication cohorts was 0.95 and 0.90, respectively. A Hardy-Weinberg equilibrium test P -value threshold of at least $P < 1 \times 10^{-6}$ was applied by each group.

Marker Selection

To reduce the computational time burden and multiple hypothesis testing, additional parallel SNP filtering steps (main effect filter and Biofilter) were employed. These strategies have been implemented by other studies as two powerful options for gene-gene interaction analysis in large-scale genotype datasets (Sun et al. 2014).

Main Effect Filter

SNPs were tested for their independent association with the continuous lipid outcome using linear regression (Asselbergs et al. 2012). SNPs with a main effect P -value < 0.01 were selected for further analysis.

Biofilter

SNPs were also analyzed using Biofilter 2.0, a knowledge-based software package that enables the analysis and identification of multi-SNP models in large datasets (Bush et al. 2009; Pendergrass et al. 2013). It has previously been used to identify predictive SNP-SNP models for traits such as age-related cataract (Hall et al. 2015), multiple sclerosis (Bush et al. 2011), HIV pharmacogenetics (Grady et al. 2011) and HDL cholesterol (Turner et al. 2011). The software combines information from various online public knowledge databases to identify genes and SNPs that are most likely to interact with each other through their mutual participation in biological processes, signaling pathways and protein-protein interactions. Biofilter also provides an *implication index*, which measures the strength of the knowledge-based support for a putative interaction model. This is indicated by the sum of the number of supporting data sources for each of the genes in a given interaction. In our analyses, we included models if they were supported by at least five sources. This was a slightly more stringent *implication index* cut-off than those used in previous studies (Turner et al. 2011).

Statistical Analyses

Covariate Adjustment

Quantitative lipid outcome values were regressed on age, sex, BMI, use of medications for lowering lipids, first ten principal components addressing population substructure, type II diabetes status and smoking status. The residual lipid outcome values from this regression model were then used as the continuous phenotypic outcome variable in QMDR analysis. Principal components were computed using EIGENSTRAT software (Price et al. 2006).

Association Analysis using QMDR

SNPs obtained from the filtering procedures described above were tested for association with the corresponding continuous lipid outcome using QMDR. QMDR is an extension of the two-class MDR algorithm used to detect and characterize multi-SNP interactions in the context of a quantitative trait (Ritchie et al. 2001; Gui et al. 2013).

Originally, the MDR algorithm was designed as a data reduction method to enable the identification of multi-locus genotype combinations that are associated with high or low risk of a disease (Ritchie et al. 2001). For a dataset of m SNPs, k SNPs can be selected to study a k -order interaction. Next, a contingency table is constructed and case-control ratios are calculated for each of the possible multi-locus genotypes for these k SNPs. The case-control ratio for each multi-locus genotype is then compared to the case-control ratio for the whole dataset. If the genotype-specific case-control ratio exceeds the case-control ratio for the dataset, it is considered to be *high-risk*, otherwise it is considered to be *low-risk*.

However, in the case of QMDR, the algorithm compares the mean value of the phenotype for a specific multi-locus genotype, to the overall mean of the phenotype within the entire dataset. Consequently, a genotype combination is considered *high-level* if its mean phenotype value is larger than the overall mean of the phenotype. Otherwise, it is considered *low-level*. Finally, QMDR combines the '*high-level*' and '*low-level*' genotypes into separate groups and compares the phenotypic outcomes between these two groups using a T-test.

QMDR also involves a 10-fold cross-validation procedure similar to the original MDR algorithm. The data is divided into 10 portions – 9 portions are used as a training dataset and the remaining portion is used as a testing dataset. The algorithm repeats the procedure described above and calculates the overall mean of the phenotype separately for the training and the testing dataset. The training t-statistic is calculated for each k -way interaction in the training dataset. Next, the k -way model with the best training score is used to predict the case-control status in the testing dataset. The training t-statistic score is used to choose the best k -order interaction model and the highest testing t-statistic is used to select the best interaction model for the dataset.

In our analyses, we used QMDR to analyze filtered SNPs for all possible SNP-SNP interaction models that are associated with a given continuous lipid outcome (HDL-C, LDL-C, TC and TG) based on their training t-statistic scores. Amongst these models, the 100 best overall SNP-SNP models were selected using their testing t-statistic scores.

Additionally, we used linear regression to adjust for the main effect of each SNP within a SNP-SNP model tested by QMDR. This was performed to increase our ability to identify pairwise interactions that are not primarily driven by the strong independent effects of the participating SNPs within a model.

Permutation testing to assess statistical significance

We also performed 1000 permutations to establish a null distribution and determine the threshold for an $\alpha=0.05$ significance level. Identical to our analysis procedure, the 100 best SNP-SNP models were selected based on their t-statistic training and testing values for each permuted dataset. The null distribution built from the 100 best SNP-SNP models from all permutations and their corresponding t-statistic values was utilized to calculate *P*-values.

Mapping SNPs to genes

SNPs within the statistically significant pairwise interactions for each quantitative lipid trait were mapped to a corresponding gene using dbSNP (build 139) and SCANDb (www.scandb.org).

Integrated Multi-Species Prediction (IMP) web server

We also used the Integrated Multi-Species Prediction (IMP) web server to query genes represented by the SNPs within identified interactions (Wong et al. 2012). IMP integrates biological evidence from multiple information sources such as experimentally verified information from gene expression studies, IntAct, MINT, MIPS, and BioGRID databases. The software mines empirical data to provide a probability score that two genes are involved in a functional and biological relationship.

Replication Analyses

SNP-SNP models with a permutation P -value < 0.05 were chosen for replication in the eMERGE dataset (McCarty et al. 2011). We also identified all SNP-SNP models that were in LD with the identified significant models. SNPs that are in high LD ($r^2 > 0.8$) with the SNPs in the interaction models, were identified using SNAP (Johnson et al. 2008). This data was used to generate a list of ‘proxy’ SNP-SNP models representing the original significant interaction models. Both the statistically significant original models and the proxy models representing them were tested for replication. Table S4 shows the number of models tested per lipid quantitative trait. Additional details of the number of LD expanded models generated and tested for each original model are presented in Table S5. The same QMDR analysis procedure was performed as described earlier.

Assessing the added variance in lipid traits explained by replicated pairwise interactions

Linear regression models were used to assess the added variance of the quantitative lipid traits explained by the SNP-SNP interactions that were replicated in our independent dataset. The reduced regression model was built by including the main effects of each of the SNPs within our replicated interactions. The full regression model included the identified pairwise interactions in addition to the terms from the reduced model. Adjusted R^2 values were used to assess the variance explained by both models. Additionally, a likelihood ratio test was used to compare both models.

Acknowledgements

CARe acknowledges the support of the National Heart, Lung and Blood Institute and the contributions of the research institutions, study investigators, field staff, and study participants in creating this resource for biomedical research (NHLBI contract number HHSN268200960009C). The IBC array data (also known as 'Cardiochip' or 'CVDSNP55v1_A' from the National Heart, Lung and Blood Institute (NHLBI) Candidate Gene Association Resource (CARe) was downloaded with appropriate permissions from the database of Genotypes and Phenotypes (dbGaP) (www.ncbi.nlm.gov/gap). The imputed genotype data for eMERGE-I and eMERGE-II can be downloaded from the database of Genotypes and Phenotypes (dbGaP) (www.ncbi.nlm.gov/gap).

Funding Statement

This work was supported by National Institutes of Health grants: NLM R01 grants (LM010098, LM011360, LM009012), GMS P20 grants (GM103506, GM103534 and GM104416), and F31 HG008588. The funders had no role in study design, data collection and analysis, decision to publish, or preparation of the manuscript.

eMERGE Network (Phase II – Year 1) Acknowledgement

The eMERGE Network was initiated and funded by the National Human Genome Research Institute (NHGRI) through the following grants: U01HG006389 (Essentia Institute of Rural Health, Marshfield Clinic Research Foundation and Pennsylvania State University); U01HG006382 (Geisinger Clinic); U01HG006375 (Group Health Cooperative/University of Washington); U01HG006379 (Mayo Clinic); U01HG006380 (Icahn School of Medicine at Mount Sinai); U01HG006388 (Northwestern University); U01HG006378 (Vanderbilt University Medical Center); and U01HG006385 (Vanderbilt University Medical Center serving as the Coordinating Center); U01HG004438 (CIDR) and U01HG004424 (the Broad Institute) serving as Genotyping Centers.

eMERGE Network (Phase I) Acknowledgement

The eMERGE Network was initiated and funded by the National Human Genome Research Institute (NHGRI), in conjunction with additional funding from the National Institute of General Medical Sciences (NIGMS) through the following grants: U01-HG-004610 (Group Health Cooperative/University of Washington); U01-HG-004608

(Marshfield Clinic Research Foundation and Vanderbilt University Medical Center); U01-HG-04599 (Mayo Clinic); U01HG004609 (Northwestern University); U01-HG-04603 (Vanderbilt University Medical Center, also serving as the Administrative Coordinating Center); U01HG004438 (CIDR) and U01HG004424 (the Broad Institute) serving as Genotyping Centers.

Competing Interests

The authors declare that no competing interests exist.

References

- Akram ON, Bernier A, Petrides F, et al (2010) Beyond LDL Cholesterol, a New Role for PCSK9. *Arterioscler Thromb Vasc Biol* 30:1279–1281. doi: 10.1161/ATVBAHA.110.209007
- Ansari KI, Kasiri S, Hussain I, et al (2012) MLL Histone Methylases Regulate Expression of HDLR-SR-B1 in Presence of Estrogen and Control Plasma Cholesterol in Vivo. *Mol Endocrinol* 27:92–105. doi: 10.1210/me.2012-1147
- Arsenault BJ, Boekholdt SM, Kastelein JJP (2011) Lipid parameters for measuring risk of cardiovascular disease. *Nat Rev Cardiol* 8:197–206.
- Asselbergs FW, Guo Y, Van Iperen EP a, et al (2012) Large-scale gene-centric meta-analysis across 32 studies identifies multiple lipid loci. *Am J Hum Genet* 91:823–838. doi: 10.1016/j.ajhg.2012.08.032
- Aung L-H-H, Yin R-X, Wu J-Z, et al (2014) Association between the MLX Interacting Protein-Like, BUD13 Homolog and Zinc Finger Protein 259 Gene Polymorphisms and Serum Lipid Levels.
- Barter PJ, Brewer HB, Chapman MJ, et al (2003) Cholesteryl Ester Transfer Protein: A Novel Target for Raising HDL and Inhibiting Atherosclerosis. *Arterioscler Thromb Vasc Biol* 23:160–167. doi: 10.1161/01.ATV.0000054658.91146.64
- Benn M, Nordestgaard BG, Jensen JS, et al (2005) Polymorphism in APOB associated with increased low-density lipoprotein levels in both genders in the general population. *J Clin Endocrinol Metab* 90:5797–5803. doi: 10.1210/jc.2005-0974
- Bild DE, Bluemke DA, Burke GL, et al (2002) Multi-ethnic study of atherosclerosis: objectives and design. *Am J Epidemiol* 156:871–81.

- Brooks MA, Dziembowski A, Quevillon-Cheruel S, et al (2009) Structure of the yeast Pml1 splicing factor and its integration into the RES complex. *Nucleic Acids Res* 37:129–143. doi: 10.1093/nar/gkn894
- Brown ML, Inazu A, Hesler CB, et al (1989) Molecular basis of lipid transfer protein deficiency in a family with increased high-density lipoproteins. *Nature* 342:448–451. doi: 10.1038/342448a0
- Bush WS, Dudek SM, Ritchie MD (2009) Biofilter: A Knowledge-Integration System for the Multi-Locus Analysis of Genome-Wide Association Studies. *Pacific Symp Biocomput* 368–379.
- Bush WS, McCauley JL, DeJager PL, et al (2011) A knowledge-driven interaction analysis reveals potential neurodegenerative mechanism of multiple sclerosis susceptibility. *Genes Immun* 12:335–340. doi: 10.1038/gene.2011.3
- Calle ML, Urrea V, Malats N, Van Steen K (2010) mbmdr: an R package for exploring gene-gene interactions associated with binary or quantitative traits. *Bioinformatics* 26:2198–9. doi: 10.1093/bioinformatics/btq352
- Cao A, Wu M, Li H, Liu J (2011) Janus kinase activation by cytokine oncostatin M decreases PCSK9 expression in liver cells. *J Lipid Res* 52:518–530. doi: 10.1194/jlr.M010603
- Dawber TR, Meadors GF, Moore FE (1951) Epidemiological approaches to heart disease: the Framingham Study. *Am J Public Health Nations Health* 41:279–81.
- Deaton C, Froelicher ES, Wu LH, et al (2011) The global burden of cardiovascular disease. *Eur J Cardiovasc Nurs* 10:S5–S13. doi: 10.1016/S1474-5151(11)00111-3
- Eichler EE, Flint J, Gibson G, et al (2010) Missing heritability and strategies for finding the underlying causes of complex disease. *Nat Rev Genet* 11:446–50. doi: 10.1038/nrg2809
- Fried LP, Borhani NO, Enright P, et al (1991) The Cardiovascular Health Study: design and rationale. *Ann Epidemiol* 1:263–76.
- Friedewald WT, Levy RI, Fredrickson DS (1972) Estimation of the concentration of low-density lipoprotein cholesterol in plasma, without use of the preparative ultracentrifuge. *Clin Chem* 18:499–502.
- Friedman GD, Cutter GR, Donahue RP, et al (1988) CARDIA: study design, recruitment, and some characteristics of the examined subjects. *J Clin Epidemiol* 41:1105–16.
- Gottesman O, Kuivaniemi H, Tromp G, et al (2013) The Electronic Medical Records and Genomics (eMERGE) Network: past, present, and future. *Genet Med* 15:761–771. doi: 10.1038/gim.2013.72
- Grady BJ, Torstenson ES, McLaren PJ, et al (2011) Use of biological knowledge to inform the analysis of gene-gene interactions involved in modulating virologic failure with efavirenz-containing treatment regimens in ART-naive ACTG clinical trials participants. *Pac Symp Biocomput* 253–264.
- Gui J, Moore JH, Williams SM, et al (2013) A Simple and Computationally Efficient Approach to Multifactor Dimensionality Reduction Analysis of Gene-Gene

Interactions for Quantitative Traits. PLoS One 8:e66545. doi: 10.1371/journal.pone.0066545

- Gundlach S, Kässens JC, Wienbrandt L (2016) Genome-wide Association Interaction Studies with MB-MDR and maxT Multiple Testing Correction on FPGAs. *Procedia Comput Sci* 80:639–649. doi: 10.1016/j.procs.2016.05.354
- Hall MA, Verma SS, Wallace J, et al (2015) Biology-Driven Gene-Gene Interaction Analysis of Age-Related Cataract in the eMERGE Network. *Genet Epidemiol* 39:376–384. doi: 10.1002/gepi.21902
- Heller DA, de Faire U, Pedersen NL, et al (1993) Genetic and Environmental Influences on Serum Lipid Levels in Twins. *N Engl J Med* 328:1150–1156. doi: 10.1056/NEJM199304223281603
- Hill C, Gerardo D, James F, et al (1989) The Atherosclerosis Risk in Communities (ARIC) Study: design and objectives. *Am J Epidemiol* 129:687–702.
- Hooper AJ, van Bockxmeer FM, Burnett JR (2005) Monogenic hypocholesterolaemic lipid disorders and apolipoprotein B metabolism. *Crit Rev Clin Lab Sci* 42:515–545. doi: 10.1080/10408360500295113
- Horton JD, Goldstein JL, Brown MS (2002) SREBPs: activators of the complete program of cholesterol and fatty acid synthesis in the liver. *J Clin Invest* 109:1125–1131. doi: 10.1172/JCI15593
- Ide T, Shimano H, Yahagi N, et al (2004) SREBPs suppress IRS-2-mediated insulin signalling in the liver. *Nat Cell Biol* 6:351–357.
- Johnson AD, Handsaker RE, Pulit SL, et al (2008) SNAP: a web-based tool for identification and annotation of proxy SNPs using HapMap. *Bioinformatics* 24:2938–9. doi: 10.1093/bioinformatics/btn564
- Kathiresan S, Melander O, Guiducci C, et al (2008a) Six new loci associated with blood low-density lipoprotein cholesterol, high-density lipoprotein cholesterol or triglycerides in humans. *Nat Genet* 40:189–197.
- Kathiresan S, Melander O, Guiducci C, et al (2008b) Six new loci associated with blood low-density lipoprotein cholesterol, high-density lipoprotein cholesterol or triglycerides in humans. *Nat Genet* 40:189–197. doi: 10.1038/ng.75
- Kathiresan S, Willer CJ, Peloso GM, et al (2009) Common variants at 30 loci contribute to polygenic dyslipidemia. *Nat Genet* 41:56–65. doi: 10.1038/ng.291
- Keating BJ, Tischfield S, Murray SS, et al (2008) Concept, design and implementation of a cardiovascular gene-centric 50 k SNP array for large-scale genomic association studies. *PLoS One* 3:e3583. doi: 10.1371/journal.pone.0003583
- Klos K, Shimmin L, Ballantyne C, et al (2008) APOE/C1/C4/C2 hepatic control region polymorphism influences plasma apoE and LDL cholesterol levels. *Hum Mol Genet* 17:2039–2046. doi: 10.1093/hmg/ddn101
- Kuivenhoven JA, de Knijff P, Boer JMA, et al (1997) Heterogeneity at the CETP Gene Locus : Influence on Plasma CETP Concentrations and HDL Cholesterol Levels . *Arterioscler Thromb Vasc Biol* 17:560–568. doi: 10.1161/01.ATV.17.3.560

- Ma L, Yang J, Runesha HB, et al (2010) Genome-wide association analysis of total cholesterol and high-density lipoprotein cholesterol levels using the Framingham heart study data. *BMC Med Genet* 11:55. doi: 10.1186/1471-2350-11-55
- Manolio TA, Collins FS, Cox NJ, et al (2009) Finding the missing heritability of complex diseases. *Nature* 461:747–53. doi: 10.1038/nature08494
- McCarty CA, Chisholm RL, Chute CG, et al (2011) The eMERGE Network: a consortium of biorepositories linked to electronic medical records data for conducting genomic studies. *BMC Med Genomics* 4:13. doi: 10.1186/1755-8794-4-13
- Middelberg RPS, Ferreira MAR, Henders AK, et al (2011) Genetic variants in LPL, OASL and TOMM40/APOE-C1-C2-C4 genes are associated with multiple cardiovascular-related traits. *BMC Med Genet* 12:123. doi: 10.1186/1471-2350-12-123
- Moore JH, Asselbergs FW, Williams SM (2010) Bioinformatics challenges for genome-wide association studies. *Bioinformatics* 26:445–55. doi: 10.1093/bioinformatics/btp713
- Nelson ER, Chang C, McDonnell DP (2014) Cholesterol and breast cancer pathophysiology. *Trends Endocrinol Metab* 25:649–55. doi: 10.1016/j.tem.2014.10.001
- Olsson AH, Volkov P, Bacos K, et al (2014) Genome-Wide Associations between Genetic and Epigenetic Variation Influence mRNA Expression and Insulin Secretion in Human Pancreatic Islets. *PLoS Genet* 10:e1004735. doi: 10.1371/journal.pgen.1004735
- Paplomata E, O'Regan R (2014) The PI3K/AKT/mTOR pathway in breast cancer: targets, trials and biomarkers. *Ther Adv Med Oncol* 6:154–166. doi: 10.1177/1758834014530023
- Pendergrass SA, Frase A, Wallace J, et al (2013) Genomic analyses with biofilter 2.0: knowledge driven filtering, annotation, and model development. *BioData Min* 6:25. doi: 10.1186/1756-0381-6-25
- Price AL, Patterson NJ, Plenge RM, et al (2006) Principal components analysis corrects for stratification in genome-wide association studies. *Nat Genet* 38:904–9. doi: 10.1038/ng1847
- Purcell S, Neale B, Todd-Brown K, et al (2007) PLINK: a tool set for whole-genome association and population-based linkage analyses. *Am J Hum Genet* 81:559–75. doi: 10.1086/519795
- Rasmussen-Torvik LJ, Pacheco JA, Wilke RA, et al (2012) High density GWAS for LDL cholesterol in African Americans using electronic medical records reveals a strong protective variant in APOE. *Clin Transl Sci* 5:394–399. doi: 10.1111/j.1752-8062.2012.00446.x
- Reymer PW, Gagne E, Groenemeyer BE, et al (1995) A lipoprotein lipase mutation (Asn291Ser) is associated with reduced HDL cholesterol levels in premature atherosclerosis. *Nat Genet* 10:28–34. doi: 10.1038/ng0595-28

- Ritchie MD (2011) Using Biological Knowledge to Uncover the Mystery in the Search for Epistasis in Genome-Wide Association Studies. *Ann Hum Genet* 75:172–182. doi: 10.1111/j.1469-1809.2010.00630.x.Using
- Ritchie MD, Hahn LW, Roodi N, et al (2001) Multifactor-dimensionality reduction reveals high-order interactions among estrogen-metabolism genes in sporadic breast cancer. *Am J Hum Genet* 69:138–47. doi: 10.1086/321276
- Soto-Ramírez N, Arshad SH, Holloway JW, et al (2013) The interaction of genetic variants and DNA methylation of the interleukin-4 receptor gene increase the risk of asthma at age 18 years. *Clin Epigenetics* 5:1. doi: 10.1186/1868-7083-5-1
- Sun X, Lu Q, Mukheerjee S, et al (2014) Analysis pipeline for the epistasis search - statistical versus biological filtering. *Front Genet* 5:106. doi: 10.3389/fgene.2014.00106
- Talmud PJ, Drenos F, Shah S, et al (2009) Gene-centric Association Signals for Lipids and Apolipoproteins Identified via the HumanCVD BeadChip. *Am J Hum Genet* 85:628–642. doi: 10.1016/j.ajhg.2009.10.014
- Teslovich TM, Musunuru K, Smith A V, et al (2010) Biological, clinical and population relevance of 95 loci for blood lipids. *Nature* 466:707–713. doi: 10.1038/nature09270
- Turner SD, Berg RL, Linneman JG, et al (2011) Knowledge-driven multi-locus analysis reveals gene-gene interactions influencing HDL cholesterol level in two independent EMR-linked biobanks. *PLoS One* 6:e19586. doi: 10.1371/journal.pone.0019586
- Verma SS, de Andrade M, Tromp G, et al (2014) Imputation and quality control steps for combining multiple genome-wide datasets. *Front Genet* 5:1–15. doi: 10.3389/fgene.2014.00370
- Voight BF, Peloso GM, Orho-Melander M, et al (2012) Plasma HDL cholesterol and risk of myocardial infarction: a mendelian randomisation study. *Lancet* 380:572–80. doi: 10.1016/S0140-6736(12)60312-2
- Wan X, Yang C, Yang Q, et al (2010) BOOST: A fast approach to detecting gene-gene interactions in genome-wide case-control studies. *Am J Hum Genet* 87:325–40. doi: 10.1016/j.ajhg.2010.07.021
- Waterworth DM, Ricketts SL, Song K, et al (2010) Genetic variants influencing circulating lipid levels and risk of coronary artery disease. *Arterioscler Thromb Vasc Biol* 30:2264–2276. doi: 10.1161/ATVBAHA.109.201020
- Weiss LA, Pan L, Abney M, Ober C (2006) The sex-specific genetic architecture of quantitative traits in humans. *Nat Genet* 38:218–222. doi: 10.1038/ng1726
- Wittekoek ME, Pimstone SN, Reymer PWA, et al (1998) A Common Mutation in the Lipoprotein Lipase Gene (N291S) Alters the Lipoprotein Phenotype and Risk for Cardiovascular Disease in Patients With Familial Hypercholesterolemia. *Circ* 97:729–735. doi: 10.1161/01.CIR.97.8.729
- Wong AK, Park CY, Greene CS, et al (2012) IMP: a multi-species functional genomics portal for integration, visualization and prediction of protein functions and networks. *Nucleic Acids Res* 40:W484-90. doi: 10.1093/nar/gks458

World Health Organization (2014) Global Status Report On Noncommunicable Diseases 2014.

Xu M, Li X, Wang J-G, et al (2005) Glucose and lipid metabolism in relation to novel polymorphisms in the 5'-AMP-activated protein kinase gamma2 gene in Chinese. *Mol Genet Metab* 86:372–378. doi: 10.1016/j.ymgme.2005.06.012

Yao J, Yan M, Guan Z, et al (2009) Aurora-A down-regulates IkappaBalpha via Akt activation and interacts with insulin-like growth factor-1 induced phosphatidylinositol 3-kinase pathway for cancer cell survival. *Mol Cancer* 8:95. doi: 10.1186/1476-4598-8-95

Figure Captions

Fig. 1 Main effect filter analysis - underlying linkage disequilibrium (LD) structure of SNPs within pairwise interactions (P -value < 0.05) associated with HDL cholesterol level. LD diagram was generated using Haploview. Interactions between SNPs are shown with dotted lines. SNPs were mapped to corresponding genes using dbSNP (build 139) and SCANDb. (rs2952101 and rs6641322 on chromosome X are not shown here)

Fig 2. Functional relationship network generated from Integrated Multi-Species Prediction (IMP) from SNP-SNP interactions associated with **(a)** HDL-C and **(b)** LDL-C after main effect filtering (P -value < 0.05). SNPs were mapped to their respective genes and used to query IMP. Nodes in the network represent genes. Orange nodes are the genes that were queried. Edges between nodes represent a functional relationship between two genes. The color of the edge signifies the strength of the relationship confidence. Known relationships are highlighted in gold

Fig. 3 Schematic design of study for the QMDR lipid traits association analysis

Supporting Information

Fig. S1 Main effect filter analysis - underlying linkage disequilibrium (LD) structure of SNPs within pairwise interactions (P -value < 0.05) associated with LDL cholesterol

level. Interactions between SNPs are shown with dotted lines. LD diagram was generated using Haploview

Fig. S2 Main effect filter analysis - underlying linkage disequilibrium (LD) structure of SNPs within pairwise interactions (P-value < 0.05) associated with total cholesterol level. Interactions between SNPs are shown with dotted lines. LD diagram was generated using Haploview

Fig. S3 Main effect filter analysis - underlying linkage disequilibrium (LD) structure of SNPs within pairwise interactions (P-value < 0.05) associated with triglyceride level. Interactions between SNPs are shown with dotted lines. LD diagram was generated using Haploview

Fig. S4 Biofilter analysis - underlying linkage disequilibrium (LD) structure of SNPs within pairwise interactions (P-value < 0.05) associated with HDL cholesterol level. Interactions between SNPs are shown with dotted lines. LD diagram showing r^2 values was generated using Haploview

Fig. S5 Biofilter analysis - underlying linkage disequilibrium (LD) structure of SNPs within pairwise interactions (P-value < 0.05) associated with LDL cholesterol level. Interactions between SNPs are shown with dotted lines. LD diagram showing r^2 values was generated using Haploview

Fig. S6 Biofilter analysis - underlying linkage disequilibrium (LD) structure of SNPs within pairwise interactions (P-value < 0.05) associated with total cholesterol level. Interactions between SNPs are shown with dotted lines. LD diagram showing r² values was generated using Haploview

Fig. S7 Biofilter analysis - underlying linkage disequilibrium (LD) structure of SNPs within pairwise interactions (P-value < 0.05) associated with triglyceride level. Interactions between SNPs are shown with dotted lines. LD diagram showing r² values was generated using Haploview

Table S1 Known biological roles of genes identified within SNP-SNP interactions associated with each lipid trait. Gene information found using GeneCards database (www.genecards.org, Accessed March 28, 2015)

Table S2 Information for cohorts providing individual level data

Table S3 Information of eMERGE cohorts providing individual level data for replication analyses

Table S4 Number of original (non-proxy) and LD-expanded (proxy) SNP-SNP models tested for replication in eMERGE dataset. Numbers are shown for each lipid trait after using both filtering methods

Table S5 Number of LD-expanded (proxy) SNP-SNP models generated for each original discovered SNP-SNP model. Also shown are the number of SNP-SNP models tested for replication in eMERGE dataset per signal. Numbers are shown for each lipid trait after using both main effect and Biofilter filtering methods

Fig. S2 Main effect filter analysis - underlying linkage disequilibrium (LD) structure of SNPs within pairwise interactions (P-value < 0.05) associated with total cholesterol level. LD diagram was generated using Haploview

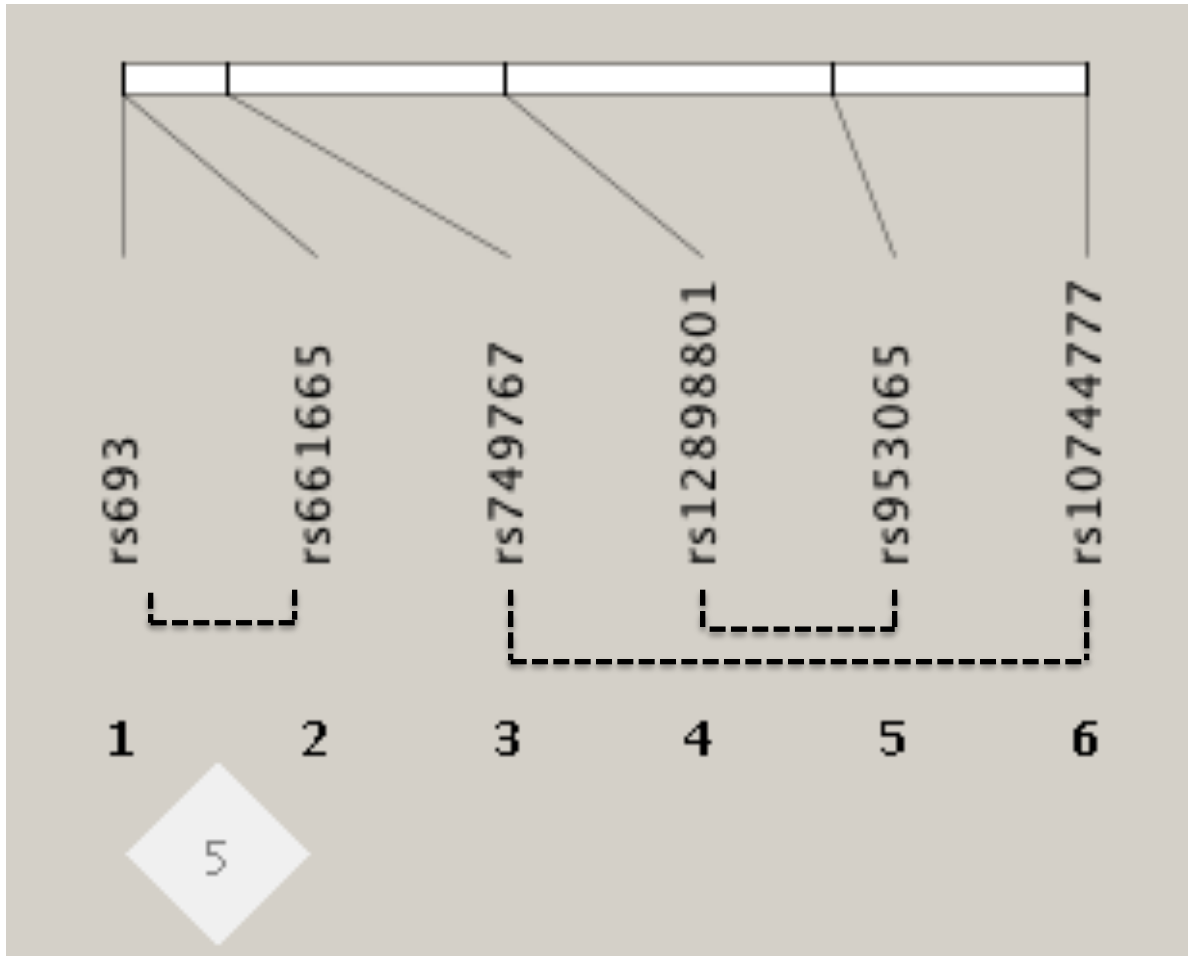


Fig. S3 Main effect filter analysis - underlying linkage disequilibrium (LD) structure of SNPs within pairwise interactions (P-value < 0.05) associated with triglyceride level. LD diagram was generated using Haploview

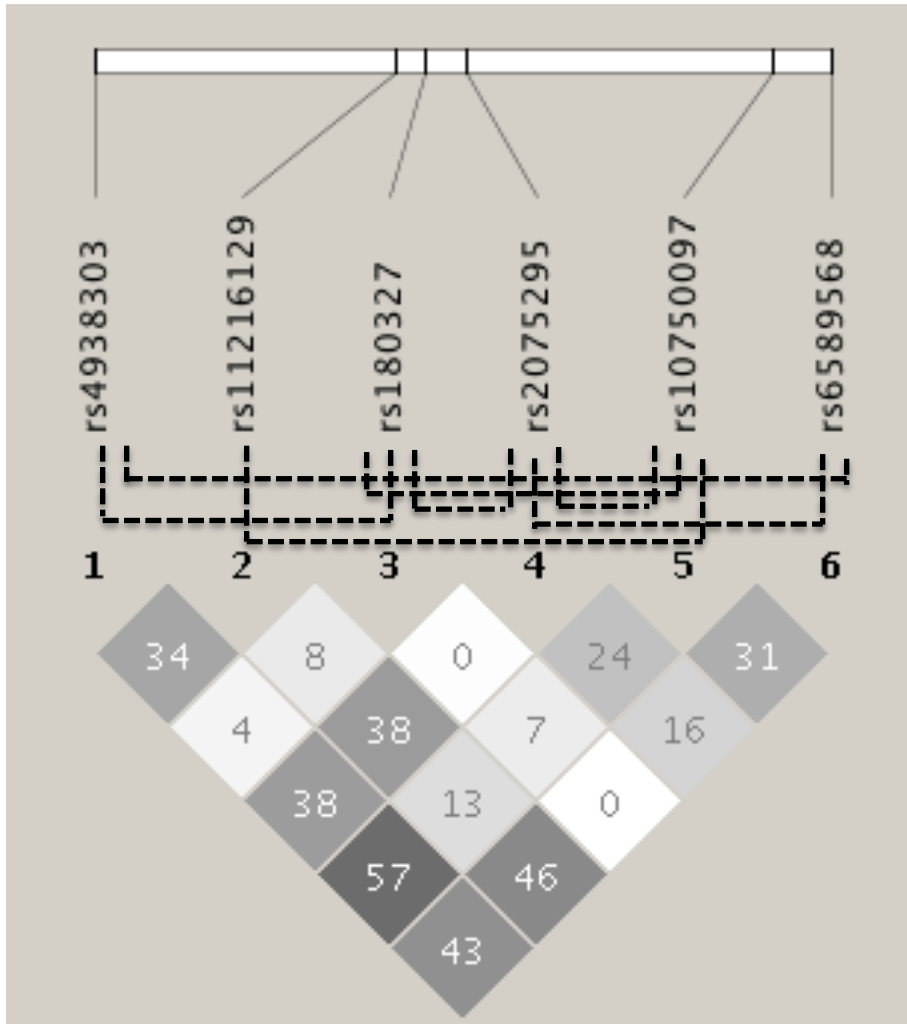


Fig. S4 Biofilter analysis - underlying linkage disequilibrium (LD) structure of SNPs within pairwise interactions (P-value < 0.05) associated with HDL cholesterol level. LD diagram showing r^2 values was generated using Haploview

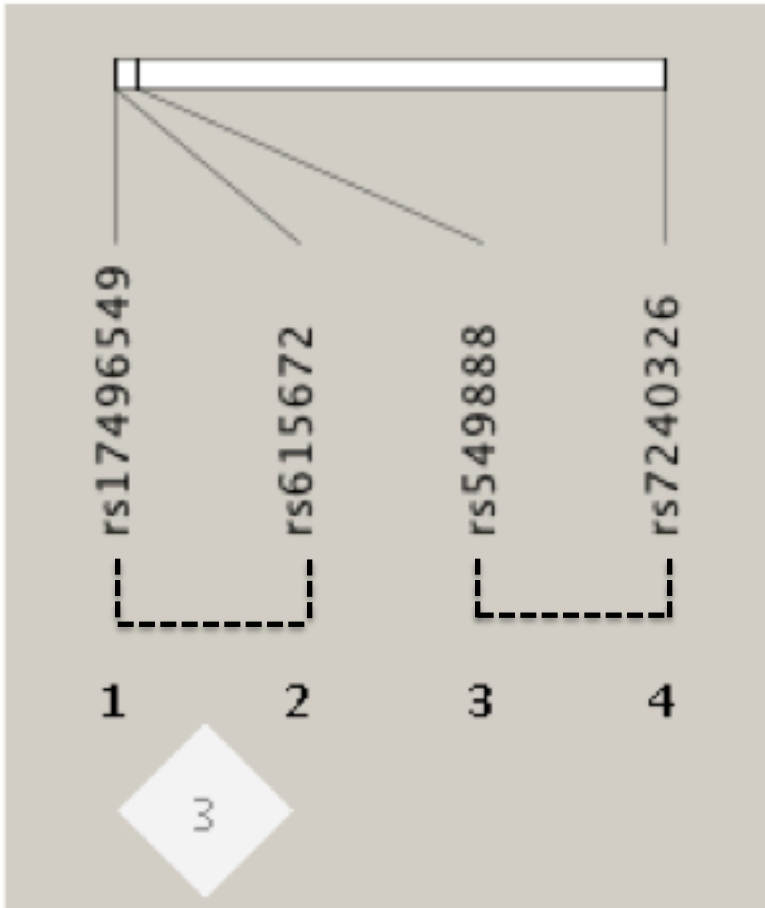


Fig. S5 Biofilter analysis - underlying linkage disequilibrium (LD) structure of SNPs within pairwise interactions (P-value < 0.05) associated with LDL cholesterol level. LD diagram showing r^2 values was generated using Haploview

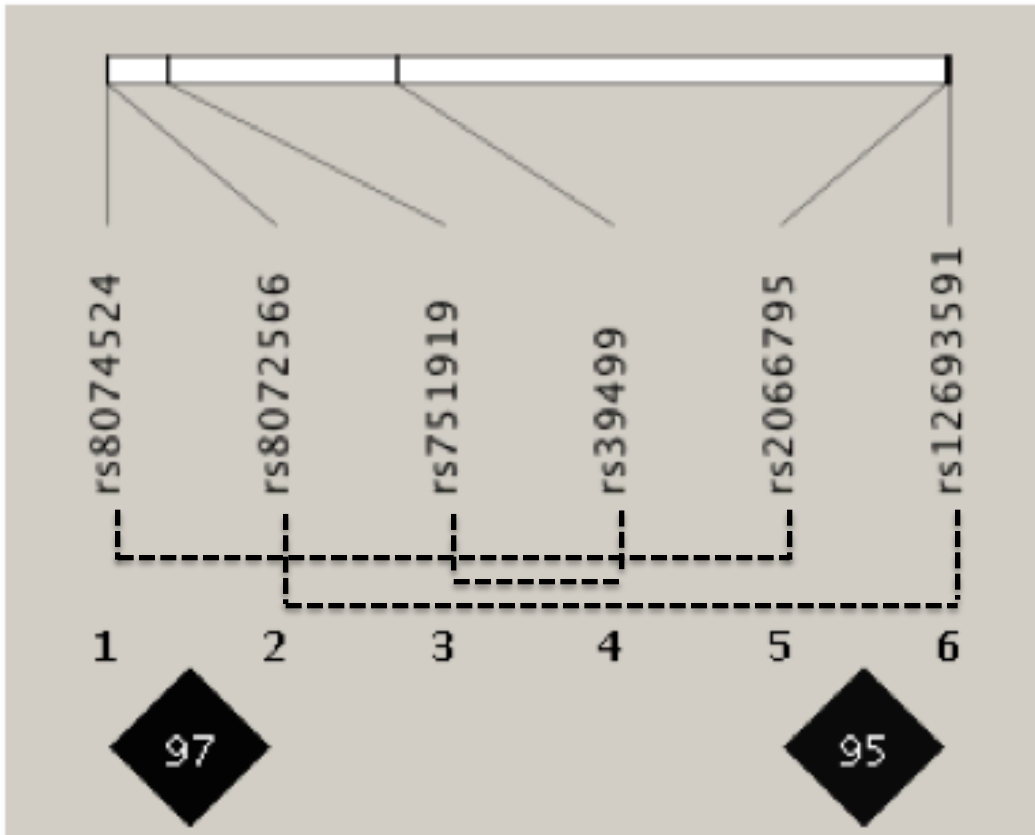


Fig. S6 Biofilter analysis - underlying linkage disequilibrium (LD) structure of SNPs within pairwise interactions (P-value < 0.05) associated with total cholesterol level. LD diagram showing r^2 values was generated using Haploview

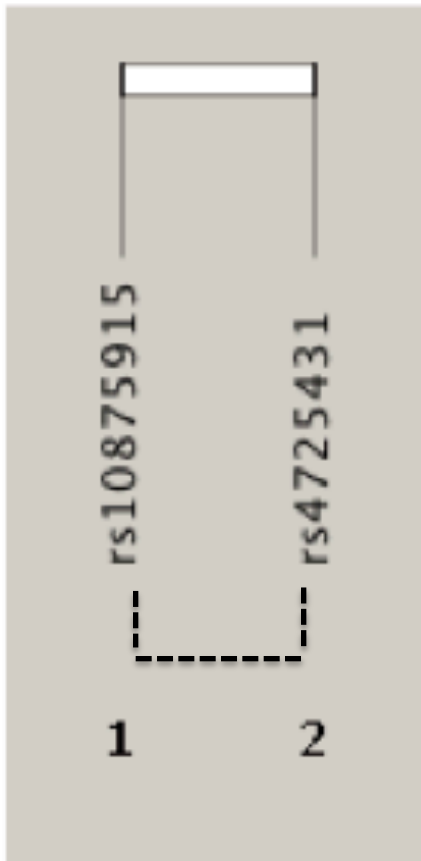


Table S1 Known biological roles of genes identified within SNP-SNP interactions associated with each lipid trait. Gene information found using GeneCards database (www.genecards.org, Accessed March 28, 2015)

Gene	Biological Role
Main effect filter: HDL-C	
CETP	Involved in the transfer of cholesteryl ester from HDL to other lipoproteins.
PDE4B	Belongs to the cyclic phosphodiesterase family. Hydrolyzes cAMP, which is a key regulator of various physiological processes.
NFKB1	Encodes for the DNA binding subunit of the NFκB complex. NFκB activates multiple immune response genes.
COX6B2	Encodes for subunit 6B2 of cytochrome C oxidase, an enzyme that is a part of mitochondrial respiration.
LPL	Mutations in LPL can cause type 1 hyperlipoproteinemia and other lipoprotein metabolism disorders.
PSRC1	Involved in microtubule dynamics and mitotic spindle organization.
DAG1	It is a part of the dystrophin-glycoprotein complex which provides a linkage between the cytoskeleton and extracellular matrix.
STAB1	Encodes for a transmembrane scavenger receptor protein that endocytoses low density lipoprotein.
MBL2	Encodes for mannose-binding lectin that is a part of the innate immune system.
FANCB	Associated with the recessive disorder Fanconi Anemia.
IDS	Mutations in this gene cause a lysosomal storage disease called Hunter syndrome.
Main effect filter: LDL-C	

TOMM40	Encodes for a membrane protein required for transport into the mitochondria. Has been associated with increased risk of Alzheimer's disease and shown to affect LDL-C levels.
C7orf10	Mutations in this gene are associated with glutaric aciduria type III.
PDE3A	Encodes for a cGMP inhibited phosphodiesterase, involved in platelet aggregation, cardiac contractility, hormone secretion, etc.
KL	Encodes for a transmembrane protein which has decreased expression in patients with chronic kidney disease
APOE	Encodes for apolipoprotein E which binds the LDL receptor and is involved in lipoprotein formation, sterol transport and cholesterol homeostasis.
CETP	Involved in the transfer of cholesteryl ester from HDL to other lipoproteins.
GATAD2A	Encodes for a zinc finger domain containing protein that acts as a transcriptional repressor. A candidate proto-oncogene, that is associated with the regulation of transcriptional activation of NFκB target genes.
BCL3	
PCSK9	Encodes for an enzyme that is an attractive drug target for hypercholesterolemia.

Main effect filter: TC

APOB	Mutations within this gene can cause an inherited form of hypercholesterolemia.
LIPC	Encodes for hepatic lipase which is involved in lipoprotein metabolism.
ALDH2	Encodes for aldehyde dehydrogenase that is involved in alcohol metabolism. Has been found to interact with genes involved in maintaining mitochondrial cholesterol levels. A polymorphism within this gene has been shown to be associated with HDL-C.
ACAN	Forms a part of the extracellular matrix in cartilagenous tissues.
BCKDK	Involved in the inactivation of a key enzyme of the valine, leucine and isoleucine catabolic pathways.

Main effect filter: TG

BUD13	Originally discovered as a splicing factor in yeast, that is involved in nuclear pre-mRNA retention.
GALNT2	Encodes for a member of the GalNAc-transferase family, that catalyzes the initial reaction in O-linked oligosaccharide biosynthesis.
FADS3	Member of the fatty acid desaturase gene family. Encodes for enzymes that regulate the unsaturation of fatty acids.
APOA5	Encodes for an apolipoprotein that maintains plasma triglyceride levels.
LIPA	Encodes for a cholesterol ester hydrolase involved in the hydrolysis of triglycerides within lysosomes.
KIAA0999	Encodes for a serine-threonine protein kinase that is a part of the SIK family.
ZNF259	Encodes for a zinc finger protein. Variants on this gene have been found to be associated with total cholesterol and triglycerides in the past.

Biofilter: HDL-C

HLA-DRA	Encodes for a member of the HLA-DR class of molecules that are a part of the major histocompatibility complex.
GGNBP1	Pseudogene of unknown function.
HLA-DRB1	Encodes for a member of the HLA-DR class of molecules that are a part of the major histocompatibility complex.
BCL2	A proto-oncogene that suppresses apoptosis. Altering cholesterol levels in the plasma membrane have been shown to affect <i>BCL2</i> gene expression.

Biofilter: LDL-C

RIPK2	Encodes for a serine-threonine kinase that is a part of the receptor interacting protein family.
-------	--

STAT1 Encodes for a transcription factor that belongs to the signal transducer and transcription activator family. It is also involved in the IL-6 signaling pathways involved in inflammation, immune regulation and oncogenesis. Oxidized LDL has been shown to activate *STAT1*.

CYLD Encodes for a cytoplasmic protein involved in ubiquitination.

STAT3 Encodes for a transcription factor that belongs to the signal transducer and transcription activator family. It is also involved in the IL-6 signaling pathways involved in inflammation, immune regulation and oncogenesis. Oxidized LDL has been shown to activate *STAT1*.

Biofilter: TC

PRKAG2 *PRKAG2* encodes for the regulatory $\gamma 2$ subunit of an AMP-activated protein kinase.

MLL2 Encodes for a mixed-lineage leukemia histone methylase.

Biofilter: TG

IRS2 Encodes for the insulin receptor substrate 2 molecule that mediates the effects of insulin.

EGFR Encodes for the epidermal growth factor receptor. Cholesterol levels in the plasma membrane have been shown to regulate *EGFR* activity.

APOA5 Encodes for an apolipoprotein that maintains plasma triglyceride levels.

INSR Encodes for the insulin receptor molecule.

GRB2 Encodes for the growth factor receptor binding protein.

KIAA0999 Encodes for a serine-threonine protein kinase that is a part of the SIK family

Table S2 Information for cohorts providing individual level data

Cohort No.	Cohort Name	Geographic Location	No. of Samples
1	ARIC	Washington County, MD; Forsyth County, NC; Jackson, MS; and Minneapolis, MN	9588
2	CARDIA	Birmingham, AL; Minneapolis, MN; Chicago, IL; and Oakland, CA	1443
4	CHS	Sacramento, CA; Hagerstown, MD; Winston-Salem, NC; and Pittsburgh, PA	3952
5	FHS	Framingham, MA	7556
6	MESA	New York, NY; Baltimore, MD; Chicago, IL; Los Angeles, CA; Twin Cities, MN; and Winston-Salem, NC	2298
Total Samples			24837

Table S3 Information of eMERGE cohorts providing individual level data for replication analyses

Site Name	Geographic Location	No. in Sample
HDL-C		
Group Health Cooperative	Seattle, WA	1861
Vanderbilt University	Nashville, TN	552
Marshfield Clinic	Stevens Point, WI	2100
Mayo Clinic	Rochester, MN	1447
Northwestern University	Evanston, IL	624
Total Sample Size		6584
LDL-C		
Group Health Cooperative	Seattle, WA	959
Vanderbilt University	Nashville, TN	578
Marshfield Clinic	Stevens Point, WI	1929
Mayo Clinic	Rochester, MN	1477
Northwestern University	Evanston, IL	553
Total Sample Size		5496

TC

Group Health Cooperative	Seattle, WA	1886
Vanderbilt University	Nashville, TN	583
Marshfield Clinic	Stevens Point, WI	2832
Mayo Clinic	Rochester, MN	1489
Northwestern University	Evanston, IL	632

Total Sample Size 7422

TG

Group Health Cooperative	Seattle, WA	1127
Vanderbilt University	Nashville, TN	586
Marshfield Clinic	Stevens Point, WI	2184
Mayo Clinic	Rochester, MN	1495
Northwestern University	Evanston, IL	625

Total Sample Size 6017

Table S4 Number of original (non-proxy) and LD-expanded (proxy) SNP-SNP models tested for replication in eMERGE dataset. Numbers are shown for each lipid trait after using both filtering methods

	No. of original SNP-SNP models tested	No. of LD-expanded models tested
Main effect filter: HDL-C	4	114
Main effect filter: LDL-C	2	23
Main effect filter: TC	0	24
Main effect filter: TG	2	15
Biofilter: HDL-C	0	3
Biofilter: LDL-C	0	305
Biofilter: TC	0	8
Biofilter: TG	8	56

Table S5 Number of LD-expanded (proxy) SNP-SNP models generated for each original discovered SNP-SNP model. Also shown are the number of SNP-SNP models tested for replication in eMERGE dataset per signal. Numbers are shown for each lipid trait after using both main effect and Biofilter filtering methods

Original discovered model	No. of additional LD expanded models generated	No. of LD-expanded models tested for replication in eMERGE
Main effect filter: HDL-C		
rs4783961,rs1800775	9	7
rs12720918,rs158477	1	0
rs4783961,rs1864163	0	1
rs12720918,rs4783961	2	0
rs1864163,rs4784744	4	3
rs12708967,rs820299	1	0
rs12447924,rs9939224	39	0
rs4783961,rs158477	0	0
rs1864163,rs158477	0	0
rs1864163,rs820299	0	0
rs4783961,rs9939224	7	1
rs1800775,rs820299	9	0
rs12744291,rs1010554	97	4
rs230541,rs4935047	159	80
rs12976922,rs2952101	7	0
rs9644636,rs7013777	25	15

rs9939224,rs4784744	39	3
rs599839,rs2952101	8	0
rs12708967,rs158477	1	0
rs3870336,rs6641322	1	0

Main effect filter: LDL-C

rs157580,rs439401	0	1
rs17435152,rs3764261	29	0
rs157580,rs405509	1	1
rs12811752,rs1469713	215	0
rs480780,rs2965174	35	21
rs625619,rs3764261	9	0

Main effect filter: TC

rs693,rs661665	31	0
rs12898801,rs953065	4	0
rs10744777,rs749767	131	24

Main effect filter: TG

rs2075295,rs6589568	0	0
rs4938303,rs180327	5	0
rs180327,rs2075295	1	2
rs180327,rs10750097	1	0
rs11216129,rs10750097	7	0
rs609526,rs12257915	20	0
rs2075295,rs10750097	0	0

rs4938303,rs6589568	2	0
rs174455,rs689243	63	11
rs180327,rs618923	3	2
Biofilter: HDL-C		
rs17496549,rs615672	51	0
rs549888,rs7240326	41	3
Biofilter: LDL-C		
rs39499,rs751919	1539	261
rs12693591,rs8072566	83	11
rs2066795,rs8074524	83	11
Biofilter: TC		
rs4725431,rs10875915	11	8
Biofilter: TG		
rs9521510,rs2860184	20	0
rs9521510,rs6510976	41	22
rs2075110,rs4789172	11	6
rs4773088,rs4804404	19	6
rs7999797,rs8109559	11	7
rs4771646,rs4804404	69	15
rs1729409,rs11216162	15	0
rs7999797,rs7252268	11	7

Additional Acknowledgements:

ARIC: The Atherosclerosis Risk in Communities Study is carried out as a collaborative study supported by National Heart, Lung, and Blood Institute contracts (HHSN268201100005C, HHSN268201100006C, HHSN268201100007C, HHSN268201100008C, HHSN268201100009C, HHSN268201100010C, HHSN268201100011C, and HHSN268201100012C), R01HL087641, R01HL59367 and R01HL086694; National Human Genome Research Institute contract U01HG004402; and National Institutes of Health contract HHSN268200625226C. The authors thank the staff and participants of the ARIC study for their important contributions. Infrastructure was partly supported by Grant Number UL1RR025005, a component of the National Institutes of Health and NIH Roadmap for Medical Research; **CARDIA:** Coronary Artery Risk in Young Adults: University of Alabama at Birmingham (N01-HC-48047, N01-HC-95095), University of Minnesota (N01-HC-48048), Northwestern University (N01-HC-48049), Kaiser Foundation Research Institute (N01-HC-48050), Tufts-New England Medical Center (N01-HC-45204), Wake Forest University (N01-HC-45205), Harbor-UCLA Research and Education Institute (N01-HC-05187), University of California, Irvine (N01-HC-45134, N01-HC-95100); **CHS:** This research was supported by contracts HHSN268201200036C, N01HC85239, N01HC55222, N01HC85079, N01HC85080, N01HC85081, N01HC85082, N01HC85083, N01HC85086, and grant HL080295 from the National Heart, Lung, and Blood Institute (NHLBI), with additional contribution from the National Institute of Neurological Disorders and Stroke (NINDS). Additional support was provided by AG023629 from the National Institute on Aging (NIA). A full list of principal CHS investigators and institutions can be found at <http://www.chs-nhlbi.org/pubs/PubAcknowGuidelines.htm>; **FHS:** The Framingham Heart Study began in 1948 with the recruitment of an original cohort of 5,209 men and women (mean age 44 years; 55 percent women). In 1971 a second generation of study participants was enrolled; this cohort consisted of 5,124 children and spouses of children of the original cohort. The mean age of the offspring cohort was 37 years; 52 percent were women. A third generation cohort of 4,095 children of offspring cohort participants (mean age 40 years; 53 percent women) was enrolled beginning in 2002. At each clinic visit, a medical history was obtained with a focus on cardiovascular content, and participants underwent a physical examination including measurement of height and weight from which BMI was calculated; **MESA:** The Multi-Ethnic Study of Atherosclerosis Study (MESA) is a multicenter prospective cohort study initiated to study the development of subclinical cardiovascular disease. A total of 6814 women and men between the age of 45 and 84 year were recruited for the first examination between 2000 and 2002. Participants were recruited in six US cities (Baltimore, MD; Chicago, IL; Forsyth County, NC; Los Angeles County, CA; Northern Manhattan, NY; and St. Paul, MN). This study was approved by the institutional review boards of

each study site, and written informed consent was obtained from all participants. This cohort was genotyped as part of the National Heart Lung and Blood Institute's (NHLBI) Candidate Gene Association Resource (CARE) (Musunuru, K., Lettre, G., Young, T., Farlow, D.N., Pirruccello, J.P., Ejebe, K.G., Keating, B.J., Yang, Q., Chen, M.H., Lapchyk, N. et al. Candidate gene association resource (CARE): design, methods, and proof of concept. *Circ. Cardiovasc. Genet*, 3, 267-275.).